4. K. Tanaka, L. M. Goldman, W. Seka, R. W. Short, and E. A. Williams, submitted to *Phys. Fluids*.

5. R. W. Short, W. Seka, K. Tanaka, and E. A. Williams, submitted to *Phys. Fluids*; LLE Review **15**, 19 (1983).

6. LLE Review **11**, 3 (1982).

7. LLE Review **14**, 3 (1983); **13**, 18 (1983).

8. K. Tanaka, L. M. Goldman, W. Seka, M. C. Richardson, J. M. Soures, and E. A. Williams, *Phys. Rev. Lett.* **48**, 1179 (1982).

9. W. Seka, E. A. Williams, R. S. Craxton, L. M. Goldman, R. W. Short, and K. Tanaka, submitted to *Phys. Fluids*.

10. A. Simon, R. W. Short, E. A. Williams, and T. Dewandre, submitted to *Phys. Fluids*.

11. V. L. Ginzburg, *The Propagation of Electromagnetic Waves in Plasmas* (Pergamon, New York, 1969).

2.C Thermal Transport and Preheat Measurements with Spherically Illuminated Targets at λ=351 nm

This section describes mass-ablation measurements obtained on OMEGA with six-beam, 351-nm irradiation of spherical targets. Diagnostics used include time-integrated x-ray spectroscopy, charge collectors, plasma calorimetry, and, on some experiments, an x-ray streak camera with a filter array. These data are also used to study the properties of thermal conduction and preheat. We review similar data obtained from 1054-nm spherical irradiation on OMEGA[1,2] and from single-beam, 351-nm irradiation on GDL.[3] These comparisons demonstrate advantages of spherical UV over IR irradiation for laser-fusion applications. As an example, the preheat of inner target layers is lower. The preheat observed in these spherical UV experiments is due to radiation from the high-Z substrate layer in the plastic (CH)-coated targets which is required to generate spectral signatures of the various preheat mechanisms. Since this radiation is not emitted until the heat front arrives at the substrate layer, the preheat can be further reduced by using a sufficiently thick plastic-overcoat layer or by avoiding the use of high-Z materials altogether. This is in contrast to the case of IR illumination where preheat has been shown to be due to hot electrons from the laser-light-absorption region which cannot be significantly attenuated by a plastic coating. Another advantage of UV illumination is that the mass-ablation rate for spherical irradiation is higher by a factor of about 1.5, as compared with spherical IR or flat-target UV irradiation for the same absorbed irradiance. Since absorption of UV light is higher than that of IR light, this factor is higher for comparisons at a fixed incident irradiance, and this factor increases with irradiance.

Previous Experiments at LLE

Figure 17.27 shows a schematic diagram of the targets and a list of the diagnostics used to study thermal transport and mass-ablation rates with six-beam, 351-nm irradiation. The time-integrated spectra

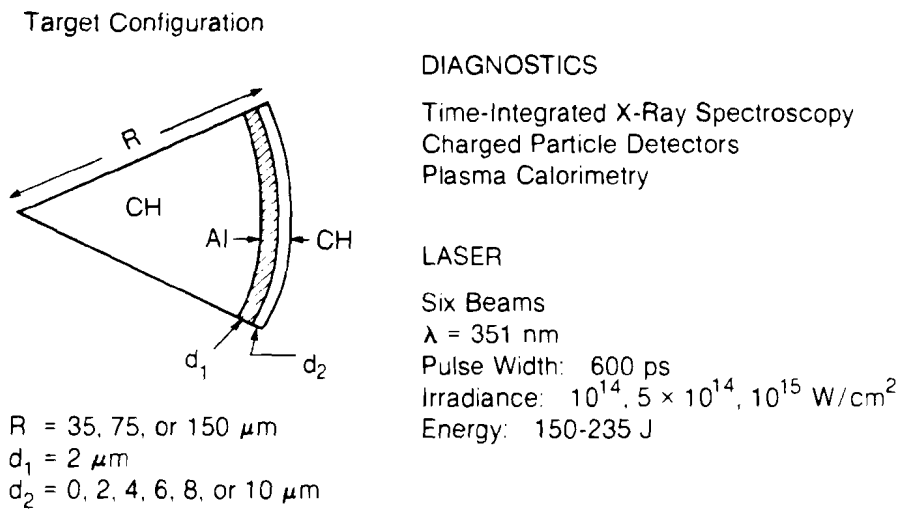

Fig. 17.27
Targets for transport "burn-through" measurements on 351-nm illuminated, uniformly irradiated spherical targets. Radiation from the Al substrate layer signals the arrival of the heat front. Other substrate materials are also used.

obtained in these studies also provide a measure of preheat as determined by K_α lines. The figure also lists the laser parameters. An x-ray streak camera with a filter array was used on some of the experiments, and these results are described below. The targets were chosen to be solid spheres so that transport and mass ablation could be studied independently of implosion and stability effects.

We first summarize the main conclusions of previous thermal-transport studies at LLE, which will be compared later with the results of new experiments with six UV beams. Experiments using a single UV beam to irradiate a plane target give "burn-through" results that agree with the predictions of a flux-limited transport model with a flux-limit parameter of f=0.03.[3] The transport measurements using 1054-nm spherical irradiation[1,2] show that the heat-front penetration, or burn-through, is about three times deeper than for non-spherical irradiation and deeper by about the same factor than the penetration predicted by the *LILAC* code for spherical irradiation and a similar flux-limited transport model. The penetration of the heat front, as measured by K lines of the high-Z substrate (Ti or Ni), is smaller by about a factor of 2 than that measured by Al K lines. Since the former lines appear at higher temperatures (1 keV and 1.5 keV, respectively) than the latter (~ 400 eV), these results imply a moderate temperature gradient at the heat front, as compared with the steep temperature profiles predicted by a flux-limited model.

These earlier experiments show that the spectroscopic determinations of ablation rates give higher values than those deduced by charge collectors. The spectroscopic diagnostics include crystal spectrographs and x-ray streak cameras. Charge-collector measurements give the ablated mass from the known absorbed energy and the expansion-velocity spectrum. The mass-ablation rate $\dot{m}$ deduced

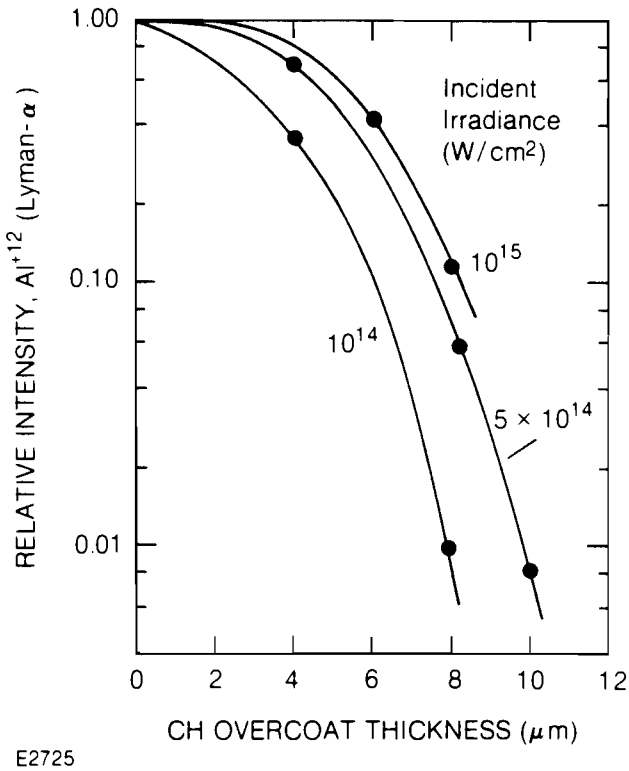

Fig. 17.28
Thermal-transport burn-through measurements using six-beam, 351-nm irradiation and CH-coated Al-substrate targets. The mass-ablation rate may be estimated by dividing the burn-through depth by the laser pulse width.

from charge collectors can be considered a lower bound, because partially ionized material is not fully weighted by charge-collector currents and is always measured to be slower than fully ionized material. These earlier experiments are described in more detail in LLE Review, Volume 13.[1]

New Burn-Through Measurements

Figures 17.28 and 17.29 show the burn-through curves obtained in the present six-beam UV experiments. Figure 17.28 gives burn-through results for plastic-coated aluminum targets, and in Fig. 17.29, aluminum is replaced by titanium. The observed spectral line intensities are plotted as functions of the plastic-coating thickness. Each curve pertains to a given irradiance at a fixed 600-ps pulse width. Each curve is separately normalized. The fall-off in intensity with increasing coating thickness shows the maximum penetration of the heat front in plastic for the given laser pulse. Since spectral line emission occurs at different temperatures, depending on the substrate material and on the chosen spectral line, such burn-through data can indicate the shape of the temperature profile of the heat front. Figure 17.30 shows the corresponding burn-through curves calculated by *LILAC* for the case of plastic-coated aluminum. The right-hand border of each band corresponds to a flux-limit parameter f=0.1, and the left-hand border corresponds to f=0.04. For an irradiance of 10^{14} W/cm^2, the two curves essentially coincide.

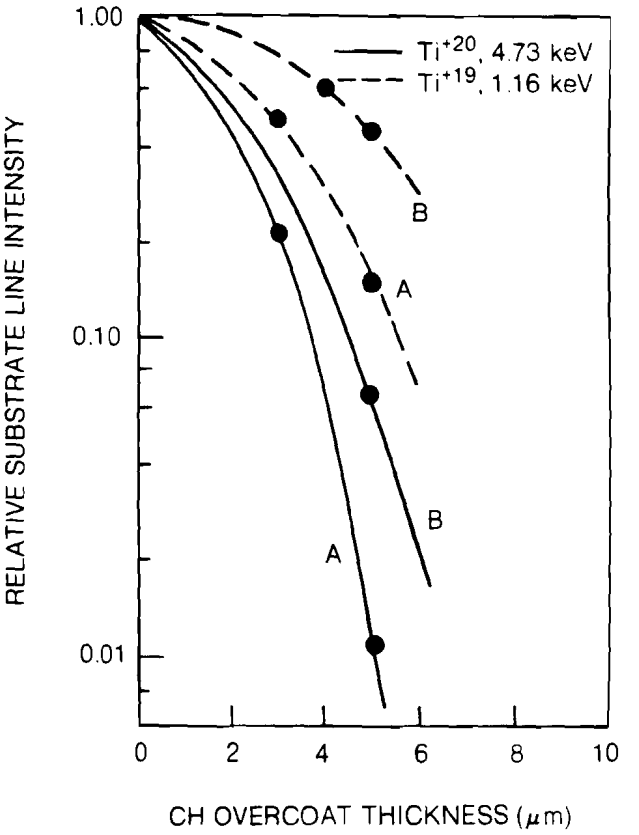

Fig. 17.29
Transport measurement in CH-coated Ti-substrate targets using six-beam, 351-nm irradiation at (a) 10^{14} W/cm^2 and (b) 5×10^{14} W/cm^2. Since the characteristic line emission of the two ion species considered is emitted at different temperatures, the difference in burn-through depths obtained for each species with a given pulse gives an indication of the scale length of the temperature profile of the heat front.

The results for 351-nm spherical irradiation are generally similar to those obtained for 1054-nm spherical irradiation. The heat front is less steep than predicted by a flux-limited model. This is evidenced by:

(a) more gradual fall-off of these curves, as compared with the predicted curves in Fig. 17.30.

(b) deeper penetration for aluminum K lines (Fig. 17.28), as compared with titanium K lines (Fig. 17.29).

(c) deeper penetration of titanium L lines (Ti^{+19}, 2p-5d transitions) as compared with titanium K lines (Ti^{+20}, $1s^2$-1s2p).

The lower-energy lines of Al^{+12} and Ti^{+19} ions generally show deeper penetration than predicted by *LILAC*. By comparing Fig. 17.28 and Fig. 17.30, we observe that the progression of penetration depth with irradiance is much slower than predicted by the code. At the irradiances of 10^{14}, 5×10^{14}, and 10^{15} W/cm^2, the measured penetration depth is larger than predicted by about a factor of 3, 2, and 1.5, respectively. With 1054-nm irradiation, this ratio is approximately 2 for the range of irradiance 5×10^{13} to 10^{15} W/cm^2.

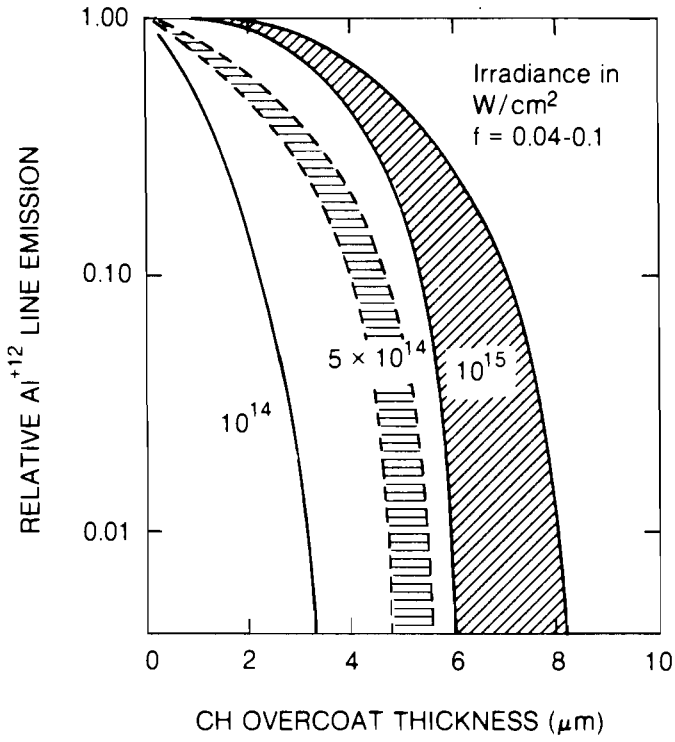

Fig. 17.30
LILAC-*calculated burn-through curves for CH-coated Al-substrate targets. The width of each band corresponds to the flux-limit-parameter range 0.04 to 0.1.*

It is important to note that the measured burn-through is deeper than that calculated for flux-limit parameter values in the range of 0.04-0.1 and that, in fact, the results cannot be explained by any value of f, especially for the lower irradiances. We have tentatively attributed these deep-penetration results to effects of long-mean-free-path (mfp) electrons, or non-local thermal transport. It is not very surprising to observe similar non-local transport effects at the two wavelengths. The importance of non-local effects to a burn-through rate has been shown to depend on the factor by which the electron mfp exceeds the temperature scale length.[4] Even though the electron mfp is shorter for UV irradiation because of the higher density in the laser-matter interaction zone, the temperature scale length in the target is also shorter at this shorter wavelength, and the mfp/scale-length ratio should not change appreciably with wavelength.

Mass-Ablation-Rate Measurements

Mass-ablation rates can be deduced from the total ablated mass, defined conservatively as the thickness which causes the substrate x-ray emission to drop by a factor of 10. After dividing the ablated mass by the laser pulse width (FWHM), we multiply by a correction factor (equal to 0.78) which relates the peak mass-ablation rate to the total ablated mass divided by the pulse width.[5] The results obtained from the aluminum data of Fig. 17.28 are shown at the top of

Fig. 17.31. This figure also shows planar-target burn-through results at 351 nm and spherical-target results at 1054 nm obtained using time-integrated and time-resolved (streak) spectral data and charge-collector data. These earlier results, including results obtained at the Rutherford Laboratory,[6] are discussed in LLE Review, Volume 13.[1]

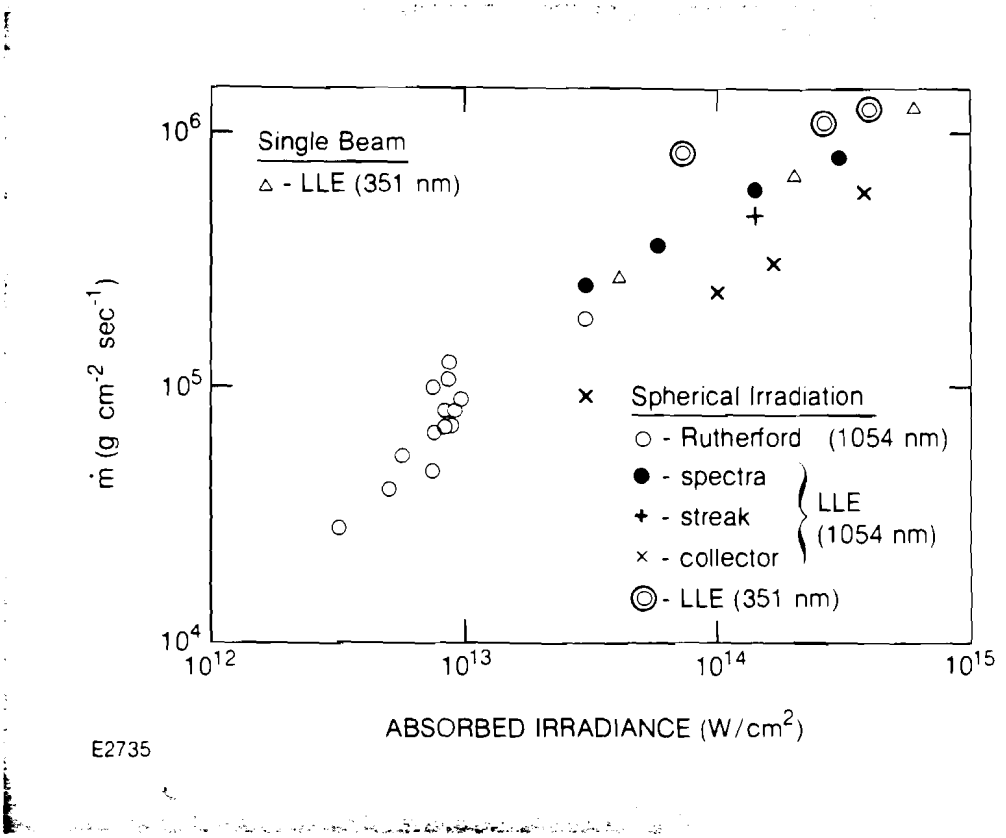

Fig. 17.31
Comparative mass-ablation rates for coated aluminum targets. Rates are obtained from spectral burn-through data and from other diagnostics. Among the new 351-nm data are data points from 1053-nm experiments performed at LLE and at the Rutherford Laboratory.[6]

The mass-ablation rates for spherical UV irradiation are higher than for either IR spherical or single-beam UV irradiation. This comparison is made for the same type of measurement in all three cases, namely, burn-through curves using the Al^{+12} Lyman-α line (1.728 keV). It should be emphasized that the comparison here and in subsequent figures is for the same absorbed irradiance. Obviously, this advantage of UV irradiation is in addition to the advantage of higher absorption; if the same comparison is made for the same incident irradiation, the advantage of UV is even more apparent.

An alternative way of determining the mass-ablation rate is by using charge-collector data which show a distinct and narrow velocity spectrum of the expanding plasma. Through this spectrum and the known absorbed energy, we derive the mass-ablation rate shown in Fig. 17.32. Again, if we compare results in UV and IR obtained in the same way (charge collectors), the rate is decidedly higher in UV than in IR. Since $\dot{m}$ is approximately given by the ratio of the absorbed irradiance and the square of the plasma velocity, this result can be stated differently: for a given absorbed irradiance, the expansion velocity is lower in UV than in IR. Indeed, the velocity corresponding to the current peak was found to follow the following

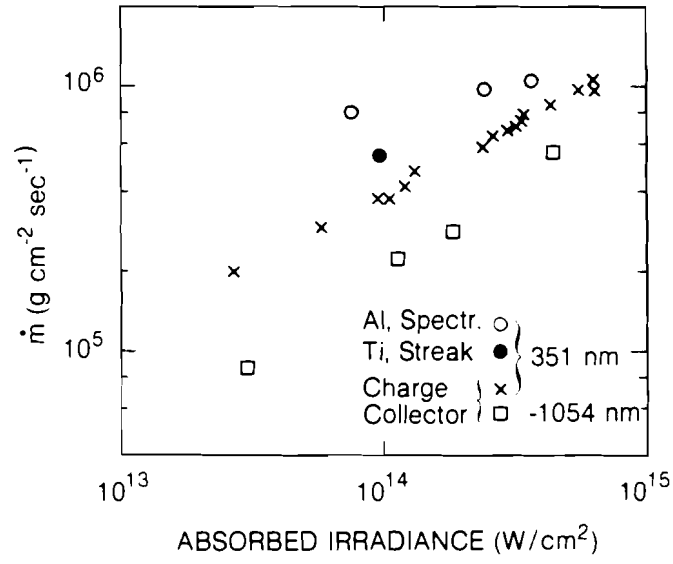

Fig. 17.32
Comparative mass-ablation rates obtained from spherical irradiation experiments. Results using various diagnostics and both aluminum and titanium substrates are compared.

scaling: $v_p = 6.9 \times 10^7\ I^{0.15}$ in UV and $v_p = 8.7 \times 10^7\ I^{0.15}$ in IR. Here, v_p is in cm/sec, and I is the absorbed irradiance in units of 10^{14} W/cm^2.

The x-ray streak camera determines $\dot{m}$ by measuring the onset time of K radiation from metal-substrate targets with various thicknesses of plastic overcoat, thus measuring the time required to ablate away a known mass of plastic. The results (Fig. 17.32) for titanium substrates are intermediate to those obtained from charge collectors and those obtained from Al^{+12} spectra. This result is consistent with spectroscopic burn-through results where titanium K radiation also indicates less penetration than does aluminum radiation (see Figs. 17.28 and 17.29).

From the mass-ablation rate, we derive the ablation pressure. The relationship usually employed is $P=\dot{m}\langle v\rangle$, where $\langle v\rangle$ is the mean expansion velocity. This relationship can only be expected to be precise to within a factor of order 1, and, indeed, code simulations show that a correction factor must be applied which lowers the pressure thus calculated by about 30%. It should be emphasized that this correction factor simply reflects internal consistency between calculating pressure through the equation of momentum conservation and the actual peak ablation pressure; the question of the correctness of the transport description in the code is of second order in importance. To be conservative, we used the $\dot{m}$ results derived from charge-collector data, which are lower than those derived from x-ray spectra. These results are shown in Fig. 17.33, compared with *LILAC* calculations for two flux-limiter values, 0.04 and 0.1. The agreement is very good. We note, incidentally, that such comparisons (and those based on streak-camera data) are not nearly as good for deducing f

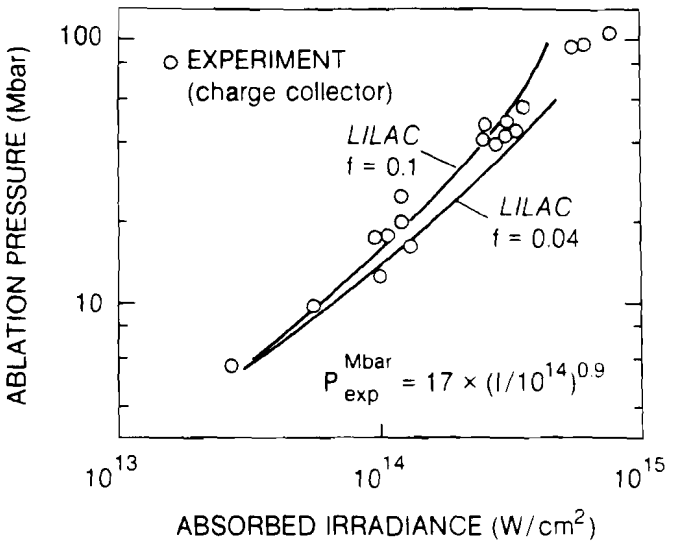

Fig 17.33
Ablation pressure in six-beam, 351-nm irradiation. Simulation results from LILAC *show good agreement over a range of flux-limit parameters.*

values as those based on burn-through curves, because the simulation results for a broad range of relevant f values fall within the scatter of the ablation-rate measurements. On the other hand, even with very large errors in measuring the intensity of the K-line radiation, the position of the steeply falling portion of the burn-through curve, and, thus, the IR penetration depth, will not be seriously in error. The precision in the abscissa (plastic thickness) is, of course, very high.

Preheat Measurements

Information on preheat can be obtained by the observation of the K_α line from cold titanium for various thicknesses of CH overcoating. For comparison, we show in Fig. 17.34 spectra obtained with 1054-nm spherical irradiation and the corresponding 351-nm data in the following figure (Fig. 17.35). The interesting thing to note in Fig. 17.34 is that in IR irradiation, the Ti^{+20} lines (coming from the hot plasma or the heat front) decay rapidly with increasing CH thickness, whereas the K_α line, which is very weak, persists in much thicker CH layers. In going from 2- to 6-μm CH thickness, the K_α line goes down in intensity by only a factor of 1.5, whereas the Ti^{+20} goes down by a factor of about 100. This occurs because the range of the fast electrons from the laser-interaction region is longer than the heat-front scale length, which allows the electrons to excite the K_α line ahead of the heat front. By comparison, Fig. 17.35 shows that with UV irradiation, the Ti^{+20} and K_α lines go down in almost exactly the same proportion as the CH thickness increases. This is a strong indication that K_α is excited by radiation emitted from the substrate as the heat-front arrives at the substrate, rather than by hot or "fast" electrons preceding the heat front. The absolute intensity of the K_α line in Fig. 17.35 is about 60

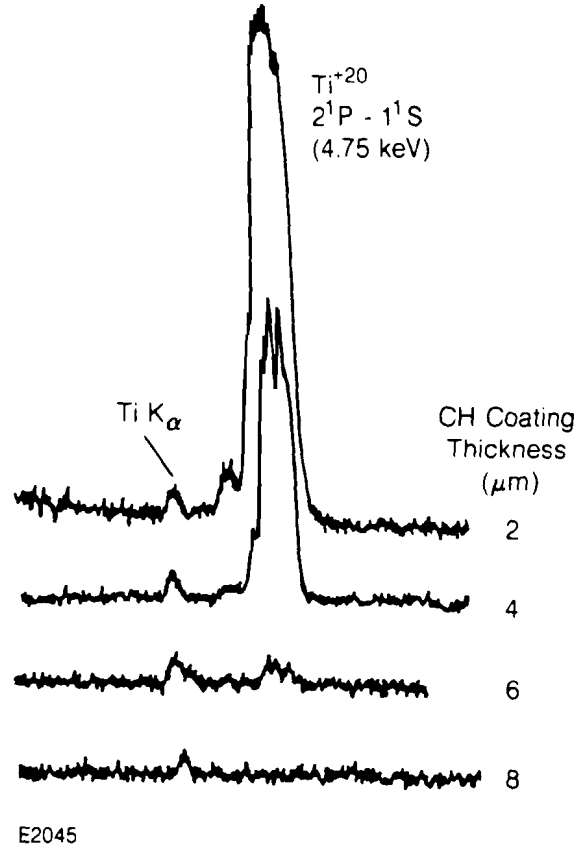

Fig. 17.34
Preheat measurement using 1054-nm irradiation and CH-coated titanium shells. The Ti^{+20} line decreases with increasing CH-layer thickness much faster than the Ti K_α radiation which persists to greater depths due to the long-range penetration of hot electrons into the cold substrate.

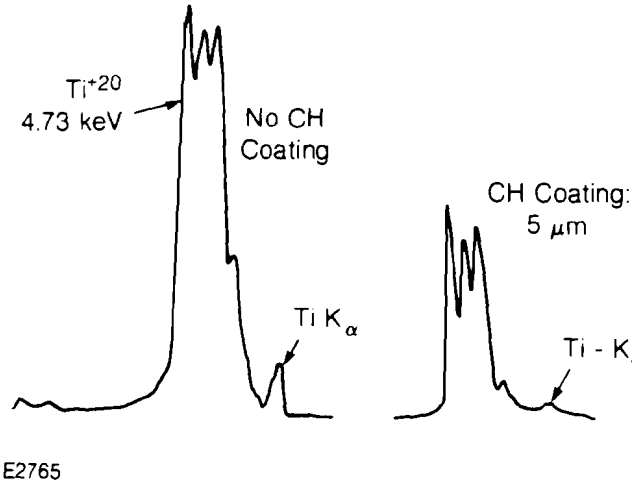

Fig. 17.35
Radiative preheat in six-beam, 351-nm irradiation. The K_α radiation is seen to decrease with increased CH coating thickness at the same rate as the Ti^{+20} lines. This suggests that the K_α radiation from colder substrate material is excited by radiation from the heated surface of the substrate.

times weaker than the Ti^{+20} resonance line, indicating only a few percent of the absorbed energy going into preheat. The important inference from these measurements is that for the UV illumination of a CH layer in the range of intensities considered, there is no measurable long-range preheat as with IR illumination. Furthermore, with CH coatings over high-Z substrates where the coating thickness is greater than the thermal penetration depth, the level of radiative preheat is extremely low.

We show in Fig. 17.36 the observed K_α intensity data plotted as a function of CH coating thickness over various substrate materials for 4×10^{14} W/cm^2 and for 1054-nm and 352-nm irradiation. The curves give theoretical predictions of the decay of electron-excited K_α intensity with increasing coating thickness, based on the expected attenuation of the hot-electron flux through the given thicknesses of plastic, for various values of the hot-electron temperature T_H. The comparison of targets with and without plastic coatings is meaningful, since the laser-energy absorption efficiency in plastic and in titanium for this irradiance is very nearly the same (50-60%), and since the dependence of T_H on the target Z is very weak. If preheat were produced by fast electrons in the UV experiment (as indeed it is in the IR experiment), the observed decay rate would correspond to the extremely low T_H value of 3 keV. The range of these hot electrons would be nearly the same as the heat-front scale length (indicated by Fig. 17.29). In this case, the hot electrons could not penetrate into the cooler, un-ionized substrate material ahead of the heat front, and there would be no possibility for K_α emission. This again supports the

Fig. 17.36
K_α measurement of the fast-electron temperature T_H using spherical 1054- and 351-nm illumination at 4×10^{14} W/cm^2. The points show the observed decay of K_α intensity with increasingly thick CH coatings. Theoretical curves for this decay at different T_H values suggest too low a T_H value for the 351-nm results to cause electron-excited K_α emission in advance of the heat front. All data and curves are normalized to unit intensity at zero coating thickness.

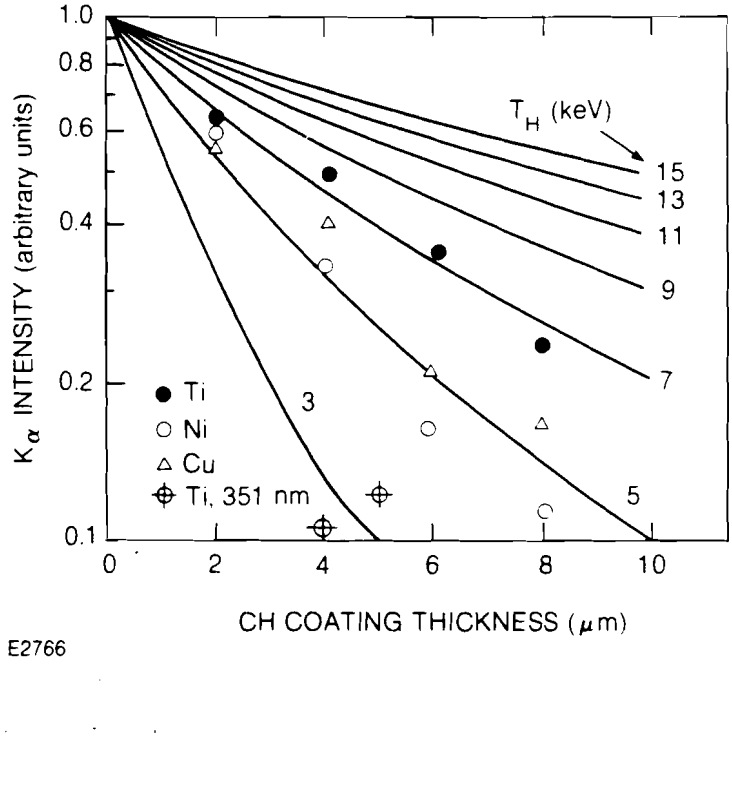

conclusion that what little preheat is indicated in Fig. 17.35 is due to titanium radiation and not due to longer-range hot electrons generated in the laser-interaction region.

Summary

Mass-ablation rates obtained with spherical UV irradiation are higher than those obtained with spherical IR irradiation at the same absorbed irradiance by a factor which varies with irradiance from 1.5 to 2.0. When this comparison is made on the basis of incident irradiance, the advantage of UV is considerably greater. The fact that mass-ablation rates derived from x-ray spectroscopic results are higher than those derived from charge-collectors suggests that complex theoretical and experimental issues in thermal-transport physics remain to be solved. Ablation pressures derived from the (more conservative) mass-ablation rates obtained from charge-collector data are consistent with numerical simulation results. The preheat levels measured by K_α emission from plastic-coated titanium targets show that the K_α line is excited primarily by x-ray radiation from the titanium and that preheat levels obtained with UV irradiation on sufficiently thick plastic coatings are less than 1% of the absorbed energy.

ACKNOWLEDGMENT

This work was supported by the U.S. Department of Energy Office of Inertial Fusion under contract number DE-AC08-80DP40124 and by the Laser Fusion Feasibility Project at the Laboratory for Laser Energetics which has the following sponsors: Empire State Electric Energy Research Corporation, General Electric Company, New York State Energy Research and Development Authority, Northeast Utilities Service Company, The Standard Oil Company, and University of Rochester. Such support does not imply endorsement of the content by any of the above parties.

REFERENCES

1. LLE Review **13**, 12 (1982).
2. B. Yaakobi, J. Delettrez, L. M. Goldman, R. L. McCrory, R. Marjoribanks, M. C. Richardson, D. Shvartz, S. Skupsky, J. M. Soures, C. Verdon, D. M. Villeneuve, T. Boehly, R. Hutchison, and S. Letzring, *Phys. Fluids* (accepted for publication).
3. B. Yaakobi, T. Boehly, P. Bourke, Y. Conturie, R. S. Craxton, J. Delettrez, J. M. Forsyth, R. D. Frankel, L. M. Goldman, R. L. McCrory, M. C. Richardson, W. Seka, D. Shvarts, and J. M. Soures, *Opt. Commun.* **39**, 175 (1981).
4. LLE Review 7, 20 (1981).
5. Rutherford Laboratory Annual Report RL-81-040, Chap. 4.4 (1981).
6. T. J. Goldsack *et al.*, *Phys. Fluids* **25**, 1634 (1982).